Quantum-Mechanical ab initio Investigation of the Transition-Metal Compounds OsO_4, OsO_3F_2, OsO_2F_4, $OsOF_6$, and OsF_8

Achim Veldkamp and Gernot Frenking*

Fachbereich Chemie der Philipps-Universität Marburg,
Hans-Meerwein-Straße, W-3550 Marburg, F.R.G.

Received August 11, 1992

Key Words: Osmium tetroxide / Osmium fluoride oxides / Osmium octafluoride / Calculations, ab initio / Pseudopotentials

The equilibrium geometries of OsO_4, OsO_3F_2, OsO_2F_4 and OsF_8 are theoretically predicted by using quantum-mechanical ab initio methods at the Hartree-Fock and MP2 level of theory employing quasi-relativistic pseudopotentials for Os and 3-21G and 6-31G(d) basis sets for O and F. A comparison of the calculated geometries and vibrational frequencies with available experimental results shows a good agreement. The energy minimum structure for OsO_4 has T_d symmetry, for OsO_3F_2 it has D_{3h} symmetry, for OsO_2F_4 C_{2v} symmetry with *cis*-coordinated oxygen atoms, and for OsF_8 a D_{2d} symmetry with two different Os−F bond lengths is predicted. $OsOF_6$ is not a minimum on the potential energy hypersurface. The calculation of the thermodynamic stabilities indicates that the Os−F bond in OsF_8 is clearly weaker than in OsO_3F_2, OsO_2F_4 and in OsF_6. It will be very difficult to observe OsF_8 experimentally. The analysis of the electronic structure shows that the Os−O bond is partly covalent, while the Os−F bonds are mainly ionic.

The highest oxidation state for any chemical element in a stable molecule is +8, and the only elements for which such compounds have been synthesized are Os, Ru and Xe. The most stable compound is OsO_4, which is an experimentally well characterized molecule[1−3]. Replacement of oxygen by fluorine atoms gives the molecules OsO_nR_{8-2n} ($n = 0-3$), which should also be good candidates for molecules with the oxidation state +8, because of the high oxidation strength of fluorine. The first member of this series, i. e. OsO_3F_2, is already known since 1957[4]. Although several spectroscopic studies have been reported in the meantime[5−7], the geometry of the molecule has yet to be determined. OsO_3F_2 has probably D_{3h} symmetry[5−7], although a fluorine-bridged structure was suggested to account for the fact that a permanent dipole moment was measured[8].

OsO_2F_4 has only recently been prepared by the reaction of OsO_4 with KrF_2[9]. A slightly distorted octahedral geometry with *cis*-coordinated oxygen atoms was found[9]. This paper[9] corrects also a previously published study in which $OsOF_6$ was identified as the reaction product[10]. All attempts to synthesize $OsOF_6$ failed[11]. Also OsF_8 has not been known so far. Earlier reports on the observation of OsF_8[12] have later been shown[13] to be due to OsF_6. There is some evidence, however, for the formation of OsF_8 by reaction of the elements at high pressure and 600°C[14].

The experimental studies of the molecules OsO_nF_{8-2n} ($n = 0-3$) are difficult because the compounds are either very reactive or may not even exist. Quantum-mechanical studies can assist experimental studies, if the theoretical results are reliable. Accurate ab initio studies have become nearly a routine for molecules containing first- and second-row elements[15] ("classical organic chemistry"), but for heavy-atom molecules such as OsO_nF_{8-2n} ($n = 0-3$) the situation is more difficult because of the large number of electrons. Pseudopotentials or effective core potential (ECP) methods could be the method of choice in this case[16]. Parameters for ECP calculations of transition-metal compounds have been developed by several groups[17−23], but little is known about the accuracy of the calculated results. In a recent systematic study of the performance of different ECP methods using various contraction schemes for the valence basis sets we found[24] that the extended ECPs developed by Hay and Wadt[17c] including the outermost $(n-1)s^2(n-1)p^6$ electrons in the valence space predict geometries for closed-shell transition-metal compounds in good agreement with experimental data. It was found that the (55/5/N)[25] minimal valence basis set should be split into [441/41/N-1,1] or, if possible, into [441/2111/N-1,1], in order to achieve good results[24]. An important finding was that the geometries of transition-metal compounds in *high* oxidation states could be calculated with good accuracy already at the Hartree-Fock level[24,26], whereas the calculation of transition-metal compounds in *low* oxidation states needs the inclusion of correlation energy in order to give reliable geometries[27,28].

In order to further test the performance of the ECP method for the theoretical study of transition-metal compounds, we calculated the geometries and the vibrational spectra of the compounds OsO_nF_{8-2n} ($n = 0-3$) using the quasi-relativistic ECP of Hay and Wadt[17c] for Os. The thermodynamic stability of the molecules is estimated by using appropriate model reactions. In order to gain insight into the electronic structure, we analyzed the computed wave function using the topological analysis developed by Bader and co-workers[29,30]

  0009−2940/93/0606−1325 $ 10.00+.25/0

Theoretical Details

The geometry optimizations and calculations of the vibrational frequencies have been carried out at different levels of theory by using the program package GAUSSIAN90[31]. First, we optimized the geometries and calculated the vibrational frequencies at the Hartree-Fock (HF) level using the quasi-relativistic ECP developed by Hay and Wadt[17c] with a split valence basis set [441/41/21] for Os and the all-electron 3–21G basis set for O and F[32]. The ECP for Os incorporates the mass-velocity and Darwin relativistic effects into the potential[17c]. This level of theory is denoted HF/I. As a next step, we optimized the geometry using the same ECP for Os[17c] but with a less contracted valence basis set [441/2111/21] in conjunction with the 6–31G(d) basis set for O and F[33]. This level of theory is denoted HF/II. The same basis sets and ECP were employed for optimizing the geometry with inclusion of correlation energy by using Møller-Plesset perturbation theory[34] terminated at second order (MP2). This is denoted MP2/II. The vibrational frequencies have been calculated at the HF/I level by using numerical second derivatives.

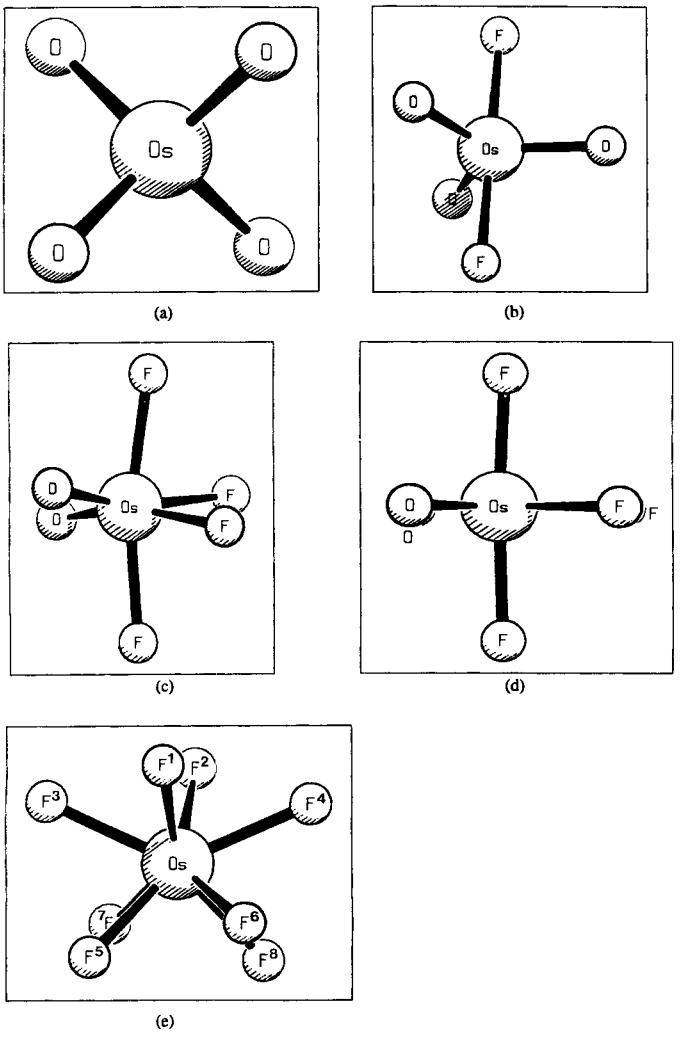

Figure 1. Optimized structures of OsO_4 (a), OsO_3F_2 (b), OsO_2F_4 at HF/I (c), OsO_2F_4 at MP2/II (d), OsF_8 at MP2/II (e)

For the calculation of the electron density distribution $\varrho(r)$, the gradient vector field $\Delta\varrho(r)$, and its associated Laplacian $\nabla^2\varrho(r)$ the programs PROAIM, SADDLE, GRID, and GRDVEC were used[35].

Results and Discussion

Figure 1 shows the optimized geometries for the calculated molecules OsO_nF_{8-2n} ($n = 0-4$). The theroretically predicted bond lengths and angles are shown in Table 1. The calculated vibrational frequencies are listed in Table 2.

Table 1. Theoretically predicted and experimentally observed bond lengths A–B [Å] and bond angles A–B–C [°]

	HF/I	HF/II	MP2/II	Exp.[a]
OsO_4:				
Symmetry	T_d	T_d	T_d	
Os–O	1.686	1.669	1.785	1.711
OsO_3F_2:				
Symmetry	D_{3h}	D_{3h}	D_{3h}	
Os–O	1.680	1.657	1.793	
Os–F	1.853	1.877	1.887	
OsO_2F_4:				
Symmetry	C_2	C_{2v}	C_{2v}	
Os–O	1.681	1.648	1.741	1.80, 1.83
$Os-F_{eq}$	1.829	1.848	1.927	1.79, 1.92
$Os-F_{ax}$	1.843	1.848	1.786	1.86, 1.88
$\alpha(O-Os-O)$	100.9	100.0	103.8	102
$\alpha(F_{eq}-Os-F_{eq})$	80.2	80.5	77.9	81
$\alpha(F_{ax}-Os-F_{ax})$	167.9	165.7	176.0	172
OsF_8:				
Symmetry	C_2	C_{2v}	D_{2d}	
$Os-F^1$	1.827	1.820	1.869	
$Os-F^3$	1.883	1.877	1.916	
$Os-F^5$	1.826	1.835		
$\alpha(F^1-Os-F^2)$	86.0	95.2	95.0	
$\alpha(F^3-Os-F^4)$	127.9	126.8	130.8	
$\alpha(F^1-Os-F^5)$	85.0	83.9	76.2	

[a] OsO_4: Ref.[2a]; OsO_2F_4: Ref.[9].

OsO_4 (T_d) is calculated at HF/I with an Os–O bond length of 1.686 Å, slightly shorter than the experimentally observed[2a] gas-phase value of 1.711 Å. The OsO_4 tetrahedron is slightly distorted in the solid state with two different Os–O distances of 1.684 Å and 1.710 Å[2c]. The calculated Os–O bond distance becomes even shorter (1.669 Å) when a better basis set is used at HF/II. With inclusion of correlation energy at MP2/II the Os–O bond length is too long (1.785 Å). This is in opposition to the theoretical results obtained for transition-metal compounds in *low* oxidation states. For example, the M–CO bond lengths in transition-metal carbonyl complexes are too long at the HF level and become even longer when the basis set is improved[28,36]. The M–CO distances become shorter and are in good agreement with experiment at the MP2 level[28]. It should be mentioned that the trend of the calculated Os–O distances, i.e. that the bond length is too short at the HF level and too long at the MP2 level, is the same as for multiple bonds of main-group elements by using standard all-electron methods[15].

The theoretically predicted vibrational frequencies at HF/I are too high, particularly for the Os–O stretching

Table 2. Theoretical predicted (at HF/I) and experimentally observed vibrational frequencies [cm^{-1}]; the calculated IR intensities [km mol^{-1}] are given in parentheses

	Mode	Frequency	Frequency × 0.8	Exp.[a]
OsO_4	T_2	342 (24.6)	274	329
	E	347 (0.0)	278	333
	T_2	1151 (140.0)	921	961
	A_1	1174 (0.0)	965	965
OsO_3F_2	E′	205 (15.2)	164	206
	A_2''	349 (66.6)	279	258
	E′	355 (8.8)	284	317
	E″	384 (0.0)	307	348
	A_1'	774 (0.0)	619	619
	A_2''	808 (198.7)	649	646
	E′	1158 (36.1)	926	929
	A_1'	1168 (0.0)	934	947
OsO_2F_4	B	97 (19.4)	78	
	A	137 (9.0)	110	
	B	157 (3.5)	126	
	A	211 (0.1)	169	
	B	297 (33.2)	238	
	A	322 (14.0)	258	
	B	394 (0.1)	315	
	A	396 (0.9)	317	
	A	443 (0.2)	354	
	B	582 (128.7)	465	
	A	765 (4.1)	612	
	B	798 (27.4)	638	
	B	836 (160.7)	669	
	A	850 (90.1)	680	
	A	1121 (14.0)	897	
OsF_8	A	107 (0.0)	86	
	B	177 (10.5)	142	
	A	213 (2.5)	170	
	B	229 (0.1)	183	
	A	320 (8.3)	256	
	A	335 (1.3)	268	
	B	374 (0.4)	299	
	B	401 (2.5)	321	
	A	440 (0.9)	352	
	B	529 (0.6)	423	
	A	553 (0.0)	442	
	B	554 (0.0)	443	
	A	564 (0.0)	451	
	A	707 (0.5)	566	
	B	717 (2.9)	574	
	A	743 (0.0)	594	
	B	751 (0.8)	601	
	A	831 (37.6)	665	
	B	840 (30.1)	672	
	A	859 (27.4)	687	
	B	864 (70.6)	691	

[a] Ref.[7].

frequencies (Table 2). This is a well-known result from calculated harmonic frequencies of main-group elements by using various basis sets[15]. With a scaling factor of 0.8 the calculated vibrational frequencies are in reasonable agreement with the experimental values[3].

The energy-minimum geometry of OsO_3F_2 is theoretically predicted to have D_{3h} symmetry (Figure 1, Table 1). This is in agreement with the structural assignment based on the infrared and Raman spectrum of OsO_3F_2[5–7]. There are no experimental values for the geometry available. The Os–O distance in OsO_3F_2 is calculated to be very similar to OsO_4 (Table 1). The Os–F interatomic distance becomes slightly longer from HF/I to HF/II and MP2/II. The theoretically predicted Os–F bond lengths are longer than the experimentally observed Os–F distance in OsF_6 (1.831 Å). The calculated vibrational frequencies are in good agreement after scaling by 0.8 with the experimental results[7].

The geometry optimization of OsO_2F_4 at HF/I yields a distorted octahedral structure with C_2 symmetry and a *cis* position of the oxygen atoms (Figure 1). The isomeric form with a *trans* position of the oxygen atoms is not a minimum on the potential energy surface, the geometry optimization gives only the structure shown in Figure 1 as an energy minimum. A *trans* position of the Os–O double bond appears not to be a stable entity. The O–Os–O plane is twisted at HF/I by 20.0° from the F–Os–F plane of the equatorial F atoms (Figure 1), and the axial fluorine atoms are slightly tilted towards the equatorial fluorine atoms with a F–Os–F bond angle of 167.9°. Reoptomization of OsO_2F_4 at HF/II and MP2/II gives a geometry with C_{2v} symmetry. A nearly perfect octahedral geometry with a bond angle F–Os–F of 176.0° for the axial fluorine atoms is predicted at MP2/II (Table 1). The experimentally observed[9] bond angles agree quite well with the calculated values. The interatomic distances show greater variations. However, the X-ray structure analysis was hampered by the poor quality of the crystals, and it was noted that rather large uncertainties remain concerning the bond lengths[9]. Also, the crystal structure of OsO_2F_4 shows a sixfold arrangement of OsO_2F_4 with a helix form which indicates that intermolecular interactions may distort the geometry of the monomer[9].

An important point concerns the relative bond lengths of the axial and equatorial Os–F bonds. At HF/I, the latter are slightly shorter than the former (Table 1). At HF/II, the two types of Os–F bonds are predicted with the same bond length. At MP2/II, the equatorial Os–F bonds are calculated significantly longer (1.928 Å) than the axial Os–F bonds (1.786 Å). Although we believe that the results obtained at MP2/II are probably correct, uncertainties remain because the experimental are not conclusive.

All attempts to find an energy minimum geometry for $OsOF_6$ failed. The molecule dissociates during the geometry optimization by using different starting geometries. We conclude that $OsOF_6$ is at best a very shallow minimum on the potential energy hypersurface, and it will be very difficult to observe it experimentally.

Unlike $OsOF_6$, osmium octafluoride OsF_8 is clearly a minimum on the potential energy hypersurface. The optimization of OsF_8 at the Hartree-Fock level using basis set I gives a distorted quadratic antiprism with C_2 symmetry as an energy-minimum structure with three different Os–F bond lengths (Figure 1). A C_{2v} structure with three different Os–F distances is predicted at HF/II. Optimization at MP2/II leads also to a distorted quadratic antiprism, but with D_{2d} symmetry and two rather long and significantly different Os–F interatomic distances of 1.916 and 1.869 Å. This is clearly longer than the Os–F bond length in OsF_6 which has experimentally been determined as 1.831 Å[37]. The calculated geometry for OsF_8 may be compared with isoelectronic $[TaF_8]^{3-}$, which has experimentally been

studied[38]. The X-ray structure analysis of the sodium salt of $[TaF_8]^{3-}$ also shows a distorted square antiprism with Ta–F bond distances ranging from 1.93 to 2.01 Å[38]. It was concluded that the departure from the ideal shape is probably caused by packing forces and the limited accuray of the X-ray structure determination, and that the $[TaF_8]^{3-}$ ion could have D_{4d} symmetry. The theoretical results presented here suggest that the departure from D_{4d} symmetry, which could be caused by a second-order Jahn-Teller distortion, may already be present in the isolated molecule.

In order to estimate the thermodynamic stability of OsF_8 and the other investigated compounds, we calculated the heats of reaction ΔH_R of the fluorination reactions (1)–(3) shown in Scheme 1.

Scheme 1. Calculated reaction enthalpies [kcal mol^{-1}] at MP2/II + ZPE; the values in parentheses are corrected by the difference in D_0 values for F_2 and O_2 [reactions (1)–(3)] and HF and H_2O [reactions (4)–(6)]

(1)	OsO_4	+ F_2	→ OsO_3F_2	+ 0.5 O_2	−55.4 (−33.7)
(2)	OsO_3F_2	+ F_2	→ OsO_2F_4	+ 0.5 O_2	−41.5 (−19.8)
(3)	OsO_2F_4	+ 2 F_2	→ OsF_8	+ O_2	−23.2 (+20.2)
(4)	OsO_4	+ 2 HF	→ OsO_3F_2	+ H_2O	+14.8 (−36.6)
(5)	OsO_3F_2	+ 2 HF	→ OsO_2F_4	+ H_2O	+27.4 (−24.0)
(6)	OsO_2F_4	+ 4 HF	→ OsF_8	+ 2 H_2O	+114.5 (+11.7)

The fluorination of OsO_4 yielding OsO_3F_2 is exothermic by 55.4 kcal mol^{-1}. This is partly due to the formation of O_2 at the expense of F_2, the bond energy of O_2 in the $^3\Sigma_g^-$ ground state is much higher (D_0 = 119.0 kcal mol^{-1})[39] than the bond energy of F_2 (D_0 = 37.8 kcal mol^{-1})[39]. If this is accounted for in reaction (1), the replacement of one Os–O double bond in OsO_4 by two Os–F single bonds increases the bond energy by 33.7 kcal mol^{-1} (Scheme 1). On the assumption that the average bond energy for the Os–O double bond in OsO_3F_2 is the same as in OsO_4 (127 kcal mol^{-1})[40] the Os–F bond strength in OsO_3F_2 can be estimated as 80.4 kcal mol^{-1}.

Further fluorination of OsO_3F_2 yielding OsO_2F_4 is also exothermic, albeit to a less extent. The theoretically predicted reaction enthalpy of reaction (2) is −41.5 kcal mol^{-1} (Scheme 1). This gives an increase in bond energy for OsO_2F_4 of 19.8 kcal mol^{-1}, when the difference in the dissociation energies of O_2 and F_2 is taken into account. Using the calculated reaction energies for reactions (1) and (2) and the Os–O bond energy[40] of OsO_4 (127 kcal mol^{-1}), we estimated the average Os–F bond strength in OsO_2F_4 as 76.9 kcal mol^{-1}, less than in OsO_3F_2.

Fluorination of OsO_2F_4 yielding OsF_8 is still exothermic by 23.2 kcal mol^{-1} (Scheme 1). However, this comes only from the formation of the oxygen molecule, the total bond energy of OsF_8 is *less* than in OsO_2F_4. If reaction (3) is corrected by the difference in the dissociation energies of F_2 and O_2, the formation of OsF_8 is endothermic by 20.2 kcal mol^{-1}. This gives together with the calculated results for reactions (1) and (2) and the Os–O bond strength[40] in OsO_4 of 127 kcal mol^{-1} a theoretically predicted Os–F bond energy of 67.7 kcal mol^{-1}, which is significantly lower than in OsO_3F_2 and OsO_2F_4. It is also much lower than the average Os–F bond energy in OsF_6 which is estimated[41] by using the results of thermodynamic measurements as 86.5 kcal mol^{-1}. The low binding energy calculated for OsF_8 may explain why this molecule could not be isolated so far.

We also calculated the formation of the fluoride oxides and OsF_8 by reaction of the precursors with HF giving the product molecules and H_2O (Scheme 1). Reactions (4)–(6) are endothermic, because in these reactions one molecule of H_2O is formed for two molecules of HF. The dissociation energy of HF is D_0 = 136.2 kcal mol^{-1}, and that of H_2O is D_0 = 221 kcal mol^{-1}[39]. If the calculated reaction enthalpies for rections (4)–(6) are corrected by the different dissociation energies of HF and H_2O, similar values are predicted for the formation of the Os–F bonds (Scheme 1). That is, the replacement of one Os–O double bond by to Os–F bonds yielding OsO_3F_2 and OsO_2F_4 gives a gain in bond energy, while the formation of OsF_8 reduces the bond energy. The two sets of reactions (1)–(3) and (4)–(6) may be used to estimate the heats of formation of OsO_3F_2, OsO_2F_4 and OsF_8. Table 3 shows the theoretically predicted[42] ΔH_f^0 values for OsO_3F_2, OsO_2F_4 and OsF_8, which have been calculated by using the experimentally observed[43] value of ΔH_f^0 (OsO_4) = −80.6 kcal mol^{-1}. The heat of formation of OsF_8 is calculated as −200.7 kcal mol^{-1} and −210.3 kcal mol^{-1}. The experimentally observed[41] heat of formation for OsF_6 is lower (ΔH_f^0 = −216 kcal mol^{-1}) which means that the dissociation of OsF_8 into OsF_6 and F_2 is probably exothermic.

In order to analyze the electronic structure of the investigated molecules, we calculated the Laplacian of the elec-

Table 3. Theoretically predicted heats of formation ΔH_f° [kcal mol^{-1}] at MP2/II + ZPE using reactions (1)–(3) and (4)–(6)

	ΔH_f°	
	Reaction (1)–(3)	Reaction (4)–(6)
OsO_3F_2	−136.0	−137.4
OsO_2F_4	−177.5	−181.6
OsF_8	−200.7	−210.3

Table 4. Characterization of bonds A–B with the aid of the local properties of energy and electron density calculated at MP2/II; shift of the bond critical point Δr_{ab} [Å] relative to the "nonpolar" midpoint of the bond A–B; electron density ϱ_b [e Å^{-3}], Laplacian concentration $\nabla^2\varrho(r_b)$ [e Å^{-5}] and energy density H_b [Hartree Å^{-3}] calculated at the bond critical point r_b

	Δr_{ab}	ϱ_b	H_b	$\nabla^2\varrho(r_b)$
OsO_4				
Os–O	+0.549	1.3592	−0.6574	24.645
OsO_3F_2				
Os–O	+0.567	1.3889	−0.7356	21.165
Os–F	+0.565	0.9833	−0.2484	18.286
OsO_2F_4				
Os–O	+0.563	1.6906	−1.2070	17.045
Os–F_{eq}	+0.591	0.9138	−0.2166	17.681
Os–F_{ax}	+0.540	1.2681	−0.4454	24.705
OsF_8				
Os–F^1	+0.583	0.9698	−0.2612	13.784
Os–F^3	+0.566	1.0522	−0.2956	18.211

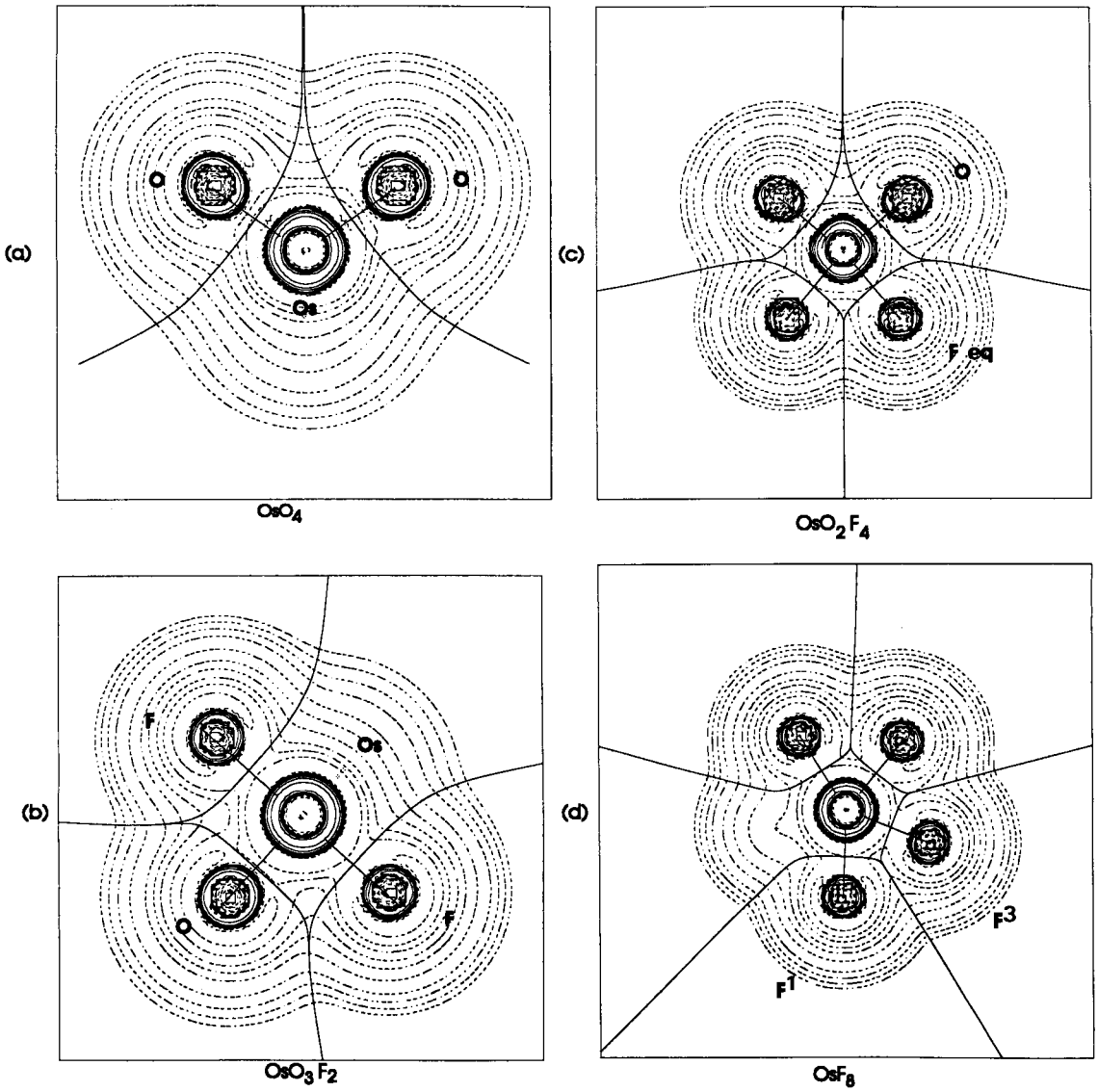

Figure 2. Contour line diagrams of the Laplacian distribution $\nabla^2\varrho(r)$ at MP2/II of OsO_4 (a), OsO_3F_2 (b), OsO_2F_4 (c), OsF_8 (d); dashed lines indicate charge depletion [$\nabla^2\varrho(r) > 0$], solid lines indicate charge concentration [$\nabla^2\varrho(r) < 0$]; the solid lines connecting the atomic nuclei are the bond paths, the solid lines separating the atomic nuclei indicate the zero-flux surfaces in the molecular plane

tron density distribution $\nabla^2\varrho(r)$ at MP2/II. Figure 2 shows the contour diagrams of the Laplacian fields, Table 4 shows the calculated results of the topological analysis of the wave function.

Inspection of the calculated contour line diagrams of the four molecules exhibited in Figure 2 shows regions of electron depletion [$\nabla^2\varrho(r) > 0$, dashed lines] and electron concentration [$\nabla^2\varrho(r) < 0$, solid lines]. The solid lines connecting the atomic nuclei are the bond paths. The solid lines separating the nuclei indicate the zero-flux surfaces in the molecular plane. The points where the solid lines are crossing between the atoms are the bond critical points r_b, which are minima of the electron density along the bond path and maxima in the two orthogonal directions[29].

Figure 2 shows that there are nearly spherical Laplace concentrations of the atoms with only small distortions caused by the electronic interactions. The calculated values for $\nabla^2\varrho(r_b)$ are always large and positive. This suggests that the Os—O and Os—F bonds should be considered as ionic. However, it has been shown that the characterization of a bond by the calculated Laplace concentration is not sufficient[44]. For example, the F—F bond in F_2 has also a positive value of $\nabla^2\varrho(r_b)$, although it is clearly a covalent bond[44a]. A better indication whether a bond is more covalent or more ionic is the energy density at the bond critical point H_b. Negative values for H_b have been shown to be a necessary and sufficient condition to characterize a bond as covalent, with typical values between -1 and -3[44,45]. The data in Table 4 show that the Os—O bond has significant covalent contributions which increase from OsO_4 to OsO_2F_4. In contrast, the Os—F bonds are largely ionic.

The shift of r_b from the "non-polar" midpoint of a bond A—B may be used as a measure of the effective electronegativity of the atoms[46]. If A and B are identical, the mid-

point is simply the half of the calculated interatomic distance. If A and B are different as in the case of the Os–O and Os–F bond, the sum of the ionic radii[47] a_{Os} and a_X, corrected by the actual interatomic distance r_{OsX}, may be used to define the "non-polar" midpoint of the Os–X bond m_{OsX}. If the latter is given by the distance to the osmium atom m_{Os}, we define m_{Os} as.

$$m_{Os} = a_{Os} \times r_{OsX} \times (a_{Os} + a_X)^{-1}$$

m_{Os} = distance of the "non-polar" midpoint from Os
a_{Os} = ionic radius of Os^{8+}
a_X = ionic radius of X (X = O^{2-}, F^-)
r_{OsX} = calculated interatomic distance Os–X

The shift in the bond critical point Δr_b is then given by the distance between r_b and m_{Os} for the Os–X bond, with negative (positive) values indicating that r_b is shifted towards the Os (X) atom. The results in Table 4 clearly show that the bond critical point r_b is alway significantly shifted towards the oxygen or fluorine atom. The position of the bond critical point r_b suggests that the electronegativity of Os^{8+} is *higher*[45] than of O^{2-} and F^-, which is in agreement with chemical intuition.

[1] For a survey on experimental studies of OsO_4 see: *Gmelin Handbuch der Anorganischen Chemie*, 8th ed., Suppl. vol. 1, Springer, Berlin, **1980**.
[2] [2a] A. Zalkin, D. H. Templeton, *Acta Crystallogr.* **1953**, *6*, 106. – [2b] H. M. Seip, R. Stølevik, *Acta Chem. Scand.* **1966**, *20*, 385. – [2c] B. Krebs, K. D. Hasse, *Acta Crystllogr., Sect. B: Struct. Crystallogr., Cryst. Chem.* **1976**, *32*, 1334.
[3] [3a] Y. M. Bosworth, R. J. H. Clark, D. M. Rippon, *J. Mol. Spectrosc.* **1973**, *46*, 240. – [3b] J. L. Huston, H. H. Claassen, *J. Chem. Phys.* **1970**, *52*, 5646. – [3c] R. S. McDowell, M. Goldblatt, *Inorg. Chem.* **1971**, *10*, 625. – [3d] C. G. Barraclough, M. M. Sinclair, *Spectrochim. Acta, Part A* **1970**, *26*, 207.
[4] M. A. Hepworth, P. L. Robinson, *J. Inorg. Nucl. Chem.* **1957**, *4*, 24.
[5] N. Nghi, N. Bartlett, *C. R. Seances Acad. Sci., Ser. C* **1969**, *269*, 756.
[6] I. R. Beattie, K. M. S. Livingstone, D. J. Reynolds, G. A. Ozin, *J. Chem. Soc. A* **1970**, 1210.
[7] I. R. Beattie, H. E. Blayden, R. A. Crocombe, P. J. Jones, J. S. Ogden, *J. Raman Spectrosc.* **1976**, *4*, 313.
[8] W. E. Falconer, F. J. Disalvo, J. E. Griffiths, F. A. Stevie, W. A. Sunder, M. J. Vasile, *J. Fluorine Chem.* **1975**, *6*, 499.
[9] R. Bougon, B. Buu, K. Seppelt, *Chem. Ber.* **1993**, *126*, 1331–1336, following paper.
[10] R. Bougon, *J. Fluorine Chem.* **1991**, *53*, 419.
[11] N. Bartlett, N. K. Jha, *J. Chem. Soc. A* **1968**, 536.
[12] O. Ruff, F. W. Tschirch, *Ber. Dtsch. Chem. Ges.* **1913**, *46*, 929.
[13] B. Weinstock, J. G. Malm, *J. Am. Chem. Soc.* **1958**, *80*, 4466.
[14] O. Glemser, H. W. Roesky, K. H. Hellberg, H. V. Werther, *Chem. Ber.* **1966**, *99*, 2652.
[15] W. J. Hehre, L. Radom, P. von Ragué Schleyer, J. A. Pople, *Ab Initio Molecular Orbital Theory*, Wiley, New York, **1986**.
[16] L. Szasz, *Pseudopotential Theory of Atoms and Molecules*, John Wiley, New York, **1985**.
[17] [17a] P. J. Hay, W. R. Wadt, *J. Chem. Phys.* **1985**, *82*, 270. – [17b] P. J. Hay, W. R. Wadt, *J. Chem. Phys.* **1985**, *82*, 284. – [17c] P. J. Hay, W. R. Wadt, *J. Chem. Phys.* **1985**, *82*, 299.
[18] [18a] Y. Sakai, E. Miyoshi, M. Klobukowski, S. Huzinaga, *J. Comput. Chem.* **1987**, *8*, 226. – [18b] Y. Sakai, E. Miyoshi, M. Klobukowski, S. Huzinaga, *J. Comput. Chem.* **1987**, *8*, 256.
[19] [19a] M. Dolg, U. Wedig, H. Stoll, H. Preuß, *J. Chem. Phys.* **1987**, *86*, 866. – [19b] D. Andrae, U. Häußermann, M. Dolg, H. Stoll, H. Preuß, *Theor. Chim. Acta* **1990**, *77*, 123.
[20] J. C. Barthelat, P. K. Durand, A. Serafini, *Mol. Phys.* **1977**, *33*, 159.
[21] L. G. M. Petterson, U. Wahlgren, O. Gropen, *Chem. Phys.* **1983**, *80*, 7.
[22] M. Krauss, W. J. Stevens, H. Basch, P. G. Jasien, *Can. J. Chem.* **1992**, *70*, 612.
[23] M. M. Hurley, L. F. Pacios, P. A. Christiansen, R. B. Ross, W. C. Ermler, *J. Chem. Phys.* **1986**, *84*, 6840.
[24] [24a] V. Jonas, G. Frenking, M. T. Reetz, *J. Comput. Chem.* **1992**, *13*, 919. – [24b] V. Jonas, G. Frenking, M. T. Reetz, *J. Comput.* **1992**, *13*, 935. – [24c] A. Veldkamp, G. Frenking, *J. Comput. Chem.* **1992**, *13*, 1184.
[25] The corresponding valence shell minimal basis sets developed by Hay and Wadt[17c] for three rows of the transition metals differ in the number of d function. The basis sets are (55/5/5), (55/5/4), and (55/5/3) for the first, second, and third row, respectively. They ares split accordingly into [441/41/41], [441/41/31], and [441,41,21].
[26] A. Neuhaus, G. Frenking, submitted for publication in *J. Am. Chem. Soc.*
[27] J. Möllman, G. Frenking, K.-H. Dötz, submitted for publication in *J. Am. Chem. Soc.*
[28] A. Ehlers, G. Frenking, to be submitted to *J. Am. Chem. Soc.*
[29] R. F. W. Bader, *Atoms in Molecules. A Quantum Theory*, Oxford Press, **1990**.
[30] [30a] R. F. W. Bader, Y. Tal, S. G. Anderson, T. T. Nguyen-Dang, *Isr. J. Chem.* **1980**, *19*, 8. – [30b] R. F. W. Bader, T. T. Nguyen-Dang, Y. Tal, *Rep. Prog. Phys.* **1991**, *44*, 893. – [30c] R. F. W. Bader, T. T. Nguyen-Dang, *Adv. Quantum. Chem.* **1981**, *14*, 63.
[31] *GAUSSIAN90*: M. J. Frisch, M. Head-Gordon, G. W. Trucks, J. B. Foreman, H. B. Schlegel, K. Raghavachari, M. A. Robb, J. S. Binkley, C. Gonzalez, D. J. DeFrees, D. J. Fox, R. A. Whiteside, R. Seeger, C. F. Melius, J. Baker, R. Martin, L. R. Kahn, J. J. P. Stewart, S. Topiol, J. A. Pople, Gaussian Inc., Pittsburgh, PA, **1990**.
[32] J. S. Binkley, J. A. Pople, W. J. Hehre, *J. Am. Chem. Soc.* **1980**, *102*, 939.
[33] W. J. Hehre, R. Ditchfield, J. A. Pople, *J. Chem. Phys.* **1972**, *56*, 2257.
[34] [34a] C. Møller, M. S. Plesset, *Phys. Rev.* **1934**, *46*, 618. – [34b] J. S. Binkley, J. A. Pople, *Int. J. Quantum Chem.* **1975**, *9S*, 229.
[35] F. W. Biegler-König, R. F. W. Bader, T. Ting-Hua, *J. Comput. Chem.* **1982**, *3*, 317.
[36] R. L. Williamson, M. B. Hall, *Int. J. Quantum. Chem., Quantum Chem. Symp.* **1987**, *21*, 503.
[37] M. Kimura, V. Schomaker, D. W. Smith, B. Weinstock, *J. Chem. Phys.* **1968**, *48*, 4001.
[38] J. L. Hoard, W. J. Martin, M. E. Smith, J. F. Whitney, *J. Am. Chem. Soc.* **1954**, *76*, 3820.
[39] *CRC Handbook of Chemistry and Physics*, CRC Press, Boca Raton, **1984**.
[40] C. Glidewell, *Inorg. Chem.* **1977**, *149*, 152.
[41] D. V. Drobot, E. A. Pisarev, *Russ. J. Inorg. Chem.* **1981**, *26*, 1.
[42] Calculated from the experimentelly observed[39] heats of formation ΔH_f^0 for HF (–64.8 kcal mol^{-1}) and H_2O (–58.0 kcal mol^{-1}). The heats of formation of F_2 and O_2 are by definition zero.
[43] D. D. Wagman, W. H. Evans, V. B. Parker, R. H. Schemm, I. Halow, S. M. Bailey, K. L. Churney, R. Nuttal, *J. Phys. Chem. Ref. Data*, **1982**, *11*, 2.
[44] [44a] D. Cremer, E. Kraka, *Angew. Chem.* **1984**, *96*, 612; *Angew. Chem. Int. Ed. Engl.* **1984**, *23*, 627. – [44b] D. Cremer, E. Kraka, *Croat. Chem. Acta* **1985**, *57*, 1265.
[45] The bond critical point r_b is the crossing point of the zero-flux surface and the bond path[29,30]. The location of r_b of a bond A–B is shifted towards A and thus, assigns a larger area of the elctronic charge to B if B is more electronegative than A.
[46] [46a] T. S. Slee, *J. Am. Chem. Soc.* **1986**, *108*, 7541. – [46b] T. S. Slee, *J. Am. Chem. Soc.* **1986**, *108*, 606. – [46c] M. Otto, S. D. Lotz, G. Frenking, *Inorg. Chem.* **1992**, *31*, 3647.
[47] The following values for the ionic radii have been taken: Os^{8+}: 0.394 Å; O^{2-}: 1.384 Å; F^-: 1.336 Å. These values are taken from *Periodensystem der Elemente*, VCH Publishers, Weinheim, **1988**.

[315/92]